ISIJ International, Vol. 48 (2008), No. 6, pp. 809–814

Effects of Heat Input and Martensite on HAZ Softening in Laser Welding of Dual Phase Steels

Mingsheng XIA,[1,2] Elliot BIRO,[3,4] Zhiling TIAN[2] and Y. Norman ZHOU[1]

1) Centre for Advanced Materials Joining, University of Waterloo, 200 University Ave. W., Waterloo, Ontario, Canada, N2L 3G1. 2) Central Iron & Steel Research Institute, 76, Xueyuan Nan Lu, Beijing, China, 100081.
3) ArcelorMittal Dofasco Inc., Box 2460, Hamilton, Ontario, Canada, L8N 3J5.
4) Department of Material Science and Engineering, McMaster University, Hamilton, Ontario, Canada.

(*Received on December 18, 2007; accepted on March 11, 2008*)

Laser welds were made in three dual-phase (DP) alloys with ultimate tensile strengths ranging from 450–980 MPa and varying microstructures to investigate effects of heat input on heat affected zone (HAZ) softening. To compare the total heat transferred into the HAZ of all the welds, heat input was normalized using the Rosenthal Equation. It was found that HAZ softening experienced in a DP steel was a function of both martensite content and heat input. Maximum HAZ softening was proportional to the martensite content, and the heat input controlled the completion of softening. Material softening was normalized by martensite content, which showed that the contribution of martensite to material hardness from the three materials is the same; however the materials had different transformation kinetics.

KEY WORDS: dual phase steels; diode laser welding; Nd:YAG laser welding; HAZ softening; martensite decomposition, Rosenthal Equation.

1. Introduction

The ongoing needs to reduce vehicular weight while increasing safety is putting stress on design due to the strength limits of conventional steels. Dual phase (DP) steels offer a promising solution to this problem as these materials have higher strength while nearly matching the formability of much lower strength steels. This family of steels differs from conventional automotive steels in that the microstructural matrix of soft ferrite is strengthened with metastable hard martensitic, and possibly bainitic, phase particles.[1] The ferrite contributes to steel ductility while the martensite determines its strength.[2] Dual phase steel is known to have greater ratio of tensile strength over yield strength than conventional high strength low alloy (HSLA) steel. The higher work hardening behavior of this material correlates to better formability and crash performance of automotive components.[3]

Previous work that studied the weldability of DP steels has concluded that in general the sub-critical area of the heat affected zone (HAZ) will soften during welding; this is typically referred to as HAZ softening.[4–7] This phenomenon is caused by tempering of the pre-existing martensite in the sub-critical areas of the HAZ.[4–7]

HAZ softening can have a significant affect on weldment strength. Transverse tensile tests on welded DP coupons also show that necking tends to initiate in this region, at stress levels that are lower than the base material strength.[4] Significant softening can also degrade the formability of welded blanks.[8] So far, no detailed or systematic study has been published to investigate the HAZ softening phenomenon of welded DP steels.

Softening of DP steels by tempering using isothermal heat treatment has been investigated extensively.[9–14] It has been suggested that martensite in DP steels tempers similarly to martensite in fully quenched low- or medium-carbon steels.[10] On the other hand, little information is available on softening of steels during non-isothermal heat treatments, such as those experienced in the subcritical area of the HAZ during welding. Some initial work has pointed out that lean alloy materials welded with higher heat input and prestrained prior to welding show increased HAZ softening in gas metal arc welds,[6] and that martensite volume fraction affects the maximum reduction of tensile strength.[15] However, systematic study of the effects of heat input and martensite content on the softening kinetics of various steels of different strengths is lacking.

In this work, the HAZ softening characteristics of three laser welded DP steels were investigated. Bead-on-plate welds were made with various speeds to vary the heat transfer into the steels and produce different severities of HAZ softening. A method was developed for normalizing the heat input with respect to laser profile and sheet thickness so that the thermal cycle applied to the various materials could be accurately compared.

2. Experimental Procedures

2.1. Materials

Experiments were done on three DP steels of different

Table 1. Dual phase steels used in this study.

	DP450	DP600	DP980
C	0.07	0.07	0.13
Mn	1.4	1.8	1.9
P	0.010	0.009	0.014
S	0.004	0.004	0.006
Si	0.04	0.10	0.03
Cr	0.5	0.0	0.2
Mo	0.0	0.2	0.3
Al_{tot}	0.04	0.04	0.06
Nb	0.00	0.00	0.00
Ti	0.00	0.01	0.00
V	0.01	0.00	0.00
N	68 ppm	116 ppm	86 ppm
CE_N	0.27	0.28	0.47
$f_{Mart\ (\%)}$	7.0	18.6	49.4
T_m (K)	1804	1803	1798
T_{Ac1} (K)	1005	993	991
Base Hardness (VHN)	162	196	283

Table 2. Characteristics of welding lasers.

Laser Machine	Laser Source	Wave Length (μm)	Power (kW)	Focal Length (mm)	Beam Size (mm)
Nuvonyx ISL-4000	Diode	0.81	4	80	0.9x12
Haas HL3006D	Nd:YAG	1.06	3	200	0.60

grades, with nominal ultimate tensile strengths of 450, 600 and 980 MPa. The chemical compositions, calculated data and mechanical properties of these steels are summarized in **Table 1**. The volume fractions of martensite (f_{Mart}) were determined using quantitative metallography after tinting with LePera's tint[16]; H_{BM} is the Vickers hardness of base metal. The carbon equivalent (CE, in wt%) has been calculated based on the formula developed by Yurioka *et al.*[17] The melting temperatures of the steels were calculated by relations found in Metals Reference Book,[18] and the Ac_1 was determined using Yurioka's relation.[19]

2.2. Laser Welding

Nd:YAG and diode lasers were used as welding heat sources. These lasers had very different beam characteristics, which allowed welding with two distinct ranges of energy input per unit length of weld, which will be referred afterwards as heat input. The Nd:YAG laser had a maximum power of 3 kW and a beam diameter of 0.6 mm. The diode laser had a maximum power of 4 kW delivered in a 0.9 mm×12 mm rectangular beam that was oriented longitudinal to the welding direction. The beam dimensions for these two lasers resulted in power densities of 10.6 kW/mm^2 and 0.67 kW/mm^2 for the Nd:YAG laser and diode laser respectively. Further details on these lasers may be found in **Table 2** It should also be noted that in laser welding, only a fraction of the incident beam energy is actually absorbed by the workpiece, due to reflection from the weld surface and/or transmission through the keyhole. Therefore, the incident power of a laser beam cannot be used directly in estimation of heat inputs or thermal cycle shapes, and an alternate procedure has been employed, which is discussed in Sec. 4.

The top surfaces of the welding coupons were shielded with high purity Ar supplied at 30 L/min. Welds were run with the lasers at full power, and heat input was varied by changing welding speed. To ensure that the HAZ properties were substantially uniform through the thickness of the welded coupons, all welds achieved full penetration.

2.3. Metallography

After welding, transverse cross sections of welds were cut, mounted and metallographically prepared with 2% nital etching solution to determine microstructure or with LePera's tint to determine martensite content.

2.4. Microhardness Testing

Vickers hardness testing was conducted on etched samples at a load of 500 g, using a dwell time of 15 s. Both the base material hardness and minimum hardness values presented are an average of 6, 3 from either side of the weld. The base material measurements were taken far from the fusion zone and the minimum hardness values were measured just outside of the intercritical temperature area in the weld HAZ. All indents were adequately spaced so that the strain fields from adjacent indents did not interfere with each other.

3. Results

All three materials, the DP450, DP600, and DP980, were welded with both the Nd:YAG and the diode laser at various welding speeds. After welding the samples were sectioned and hardness tested. The resulting hardness profiles were typical of those reported in many past studies.[4,6] Typical hardness traces for this study are shown in **Fig. 1**.

3.1. Effects of Laser Welding on Weld Metal Hardness

The two sets of hardness profiles in Fig. 1 show patterns that indicate how both laser type and material affect the weld hardness profiles. When the profiles from the Nd:YAG laser (Fig. 1(a)) are compared to those made by the diode laser (Fig. 1(b)) it may be seen that the Nd:YAG laser produced harder welds. For example the DP600 had a weld hardness of 396 VHN and 322 VHN when welded with the Nd:YAG and diode laser respectively. This is expected because of the higher linear heat input of the diode laser. However, it should be noted that the welds in the DP980 had approximately the same hardness when welded with both lasers. This is due to its high CE, which allowed it to fully transform to martensite even at the slower cooling rate experienced when welded with the diode laser. Likewise, as base metal strength increased, the hardness of the laser welds also increased. This is also expected because the strengthening mechanism of the materials used in this study depends on hard transformation products, and the higher strength materials had more hardenability-promoting alloying additions so they formed more martensite after welding with the same parameters.

3.2. Effects of Laser Welding on HAZ Softening

Of more interest to this study was the changes noticed between the softening behaviour of these welds. As observed in previous studies, the maximum softening was noted at the microstructural area of the HAZ where the peak temperature during correlated to the steel's Ac_1 temperature.[15] As may be seen in Fig. 1 both the laser type and material affected softening behaviour. Of the welds made with the Nd:YAG laser only the DP980 exhibited any soft-

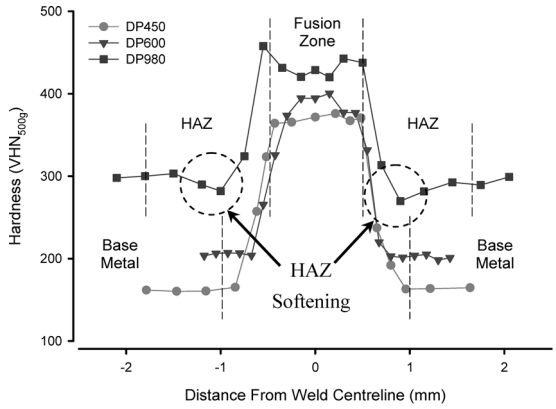

(a)

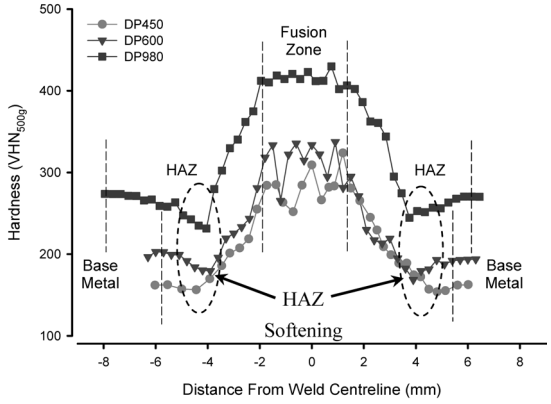

(b)

Fig. 1. Hardness profiles across welds: (a) Nd:YAG laser welding with speed of 6.0 m/min and (b) diode laser welding with speed of 1.3 m/min

ening (see Fig. 1(a)). Conversely, Fig. 1(b) shows that all of the materials welded with the diode laser softened to various degrees in the weld HAZ: 7 VHN for the DP450, 18 VHN for the DP600, and 50 VHN for the DP980. It also should be noted that the degree of softening is correlated to material strength. This is due to the influence of martensite content on the strength of these materials. As was previously reported[15] the decrease in physical properties is greater at higher martensite contents.

3.3. Effects of Welding Speed on Minimum HAZ Hardness

To further examine the effects of welding heat on HAZ softening, the minimum HAZ hardnesses of all of the welds were graphed against welding speed. The summary of minimum HAZ hardness seen in **Fig. 2** matches the softening effects of laser type and material seen in Fig. 1, but Fig. 2 also shows that that softening increases as welding speed is reduced, and at very high welding speeds very little reduction in hardness occurs. As well, it should be noted that the HAZ hardnesses of diode laser welds are lower than those of the Nd:YAG welds for each grade.

The HAZ softened region becomes smaller in width and depth as welding speed increases due to the reduced heat input at higher welding speeds. The reduced heat input

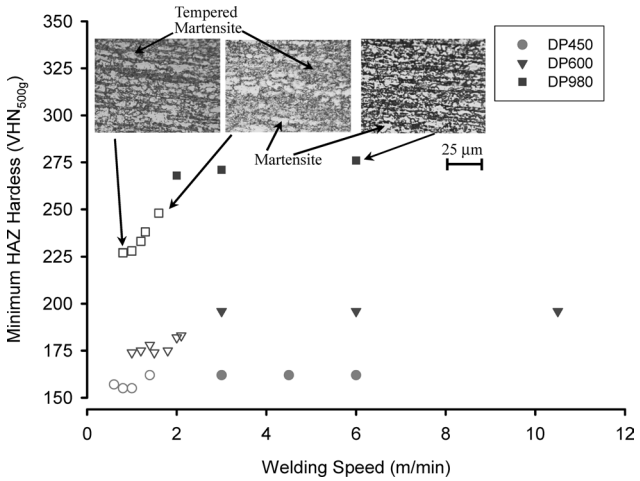

Fig. 2. Minimum hardness at Ac_1 *versus* welding speed and representative micrographs. Etchant: LePera's tint.

shortens the thermal cycle so that it cannot fully temper the martensite in the dual phase steels. Increasing tempering with increasing heat input was also confirmed by examining the representative microstructures at various welding speeds. At high welding speeds the martensite at the AC_1 area of the HAZ remained white after etching indicating that minimal sub-microscopic carbides had precipitated (see Fig. 2). Then at slower welding speeds it was found that the former martensite grains became progressively more grainy and darker after etching indicating greater carbide growth, *i.e.* more complete tempering.

Because of the observed correlation between welding speed and tempering, a method was sought to characterize the tempering kinetics responsible for HAZ softening. Because of the difference in the heating profiles of the Nd:YAG and diode laser and the varying fraction of absorbed laser energy, the hardness values of the various welds could not be readily compared. It was found that comparison of the softening behaviours of these steels and the different welding processes was best accomplished on a basis of heat input.

4. Discussion

4.1. Normallizing Heat Input from Welds Using the Rosenthal Equation

To properly compare the effects of Nd:YAG and diode laser welding on the HAZ hardness, the two processes must be compared so that the effects of beam geometry are excluded from the analysis. Because this work has examined the results of martensite tempering, which is affected by time and temperature, the analysis had to consider effects on actual thermal cycle shape, which was best done by examining the heat input. As noted in Sec. 3.2 the maximum softening occurs where the peak temperature during welding reaches the material's Ac_1. The Ac_1 temperatures for all of the studied steels were within 14°C of each other (see Table 1). So it was reasonable to treat the Ac_1 temperatures of these grades as being equal. This simplified the tempering analysis to a calculation of the relative tempering time at each material's respective Ac_1 temperature.

Although it is accepted that the Rosenthal heat conduc-

tion equations poorly model fusion zone temperature and shape because they cannot account for varying material properties or convective heat transfer, these deficiencies are not significant in the HAZ far away from the weld. In fact, Ashby and Easterling as well as Ion *et al.* were able to effectively use a Rosenthal formulation to predict grain growth and martensite development in the HAZ[20,21] by calculating the hold times at temperatures of interest. The analysis proposed here employs the models used by those authors.

The following analysis applies Rosenthal's solution for a fast moving power source on a thin plate to the problem of analyzing welding speed effects in these experiments independent of beam geometry. The two-dimensional analysis was used in favour of the three-dimensional analysis as all of the welds fully penetrated the base material. The temperature profile in the HAZ may therefore be described as[22]:

$$T - T_0 = \frac{Q_{\text{net}}/(vd)}{\rho c(4\pi at)^{1/2}} \exp\left(-\frac{r^2}{4at}\right) \quad \text{.....(1)}$$

where T_0 is the initial (ambient) temperature, about 298 K, Q_{net} is the net laser power (W), v is welding speed (mm/s), d is sheet thickness (mm), ρ is the density of steel (7 860 kg/m^3), c is the specific heat capacity of steel (680 J/kg/K), λ is the thermal conductivity (30 W/m/K), a is the thermal diffusivity ($\lambda/\rho c$), t is time (s), and r is the transverse direction (mm). $Q_{\text{net}}/(vd)$ is the thickness-normalized net absorbed energy per unit weld length, commonly referred to as "heat input".

As this study is focused on the location of the HAZ where the maximum temperature during welding reached the AC_1, Eq. (1) may be simplified by solving for the peak temperature as was done by Ashby and Easterling[21]:

$$T_{\text{P}} - T_0 = \frac{Q_{\text{net}}/vd}{\rho c r(2\pi e)^{1/2}} \quad \text{.....(2)}$$

Eq. (2) may be rearranged to determine $Q_{\text{net}}/(vd)$ by substituting the direct measurements from the weld cross section (see **Fig. 3**) into the Eq. (3)

$$\frac{Q_{\text{net}}}{vd} = \frac{\rho c(r_{\text{Ac}_1} - r_{\text{m}})(2\pi e)^{1/2}}{\left(\dfrac{1}{T_{\text{Ac}_1} - T_0} - \dfrac{1}{T_{\text{m}} - T_0}\right)} \quad \text{.....(3)}$$

where, r_{Ac1} and r_{m} are the isotherm positions corresponding to the T_{Ac1} and T_{m} (melting temperature), respectively, and can be measured experimentally from the weld cross sections.

Once the laser heat input for each weld is calculated, it may be used to calculate a time constant representing the time required to heat the base material to its Ac_1 temperature. This can be derived from the time derivative of Eq. (1) at the peak temperature ($dT/dt=0$):

$$\tau = \frac{1}{4\pi e\lambda\rho c} \frac{[Q_{\text{net}}/(vd)]^2}{(T_{\text{Ac}_1} - T_0)^2} \quad \text{.....(4)}$$

This time constant was found to be appropriate for comparing tempering times of two welds. An increase in the time needed to heat the HAZ to the Ac_1 directly corresponds to increase in the time for which this region of the HAZ will remain at temperatures sufficient to temper the martensite within the material's microstructure. The time constant as defined above was found to be directly applicable to compare the heat input delivered by the Nd:YAG and diode lasers. Because this procedure calibrates the net absorbed laser power by measuring isotherm positions, it is also able to substantially correct for the differences in laser beam shape.

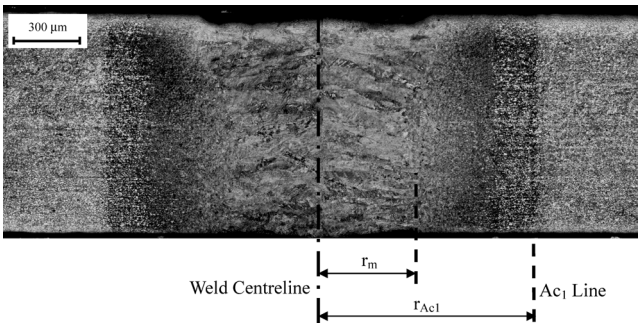

Fig. 3. Cross section of a DP600S diode laser weld with speed of 1.4 m/min.

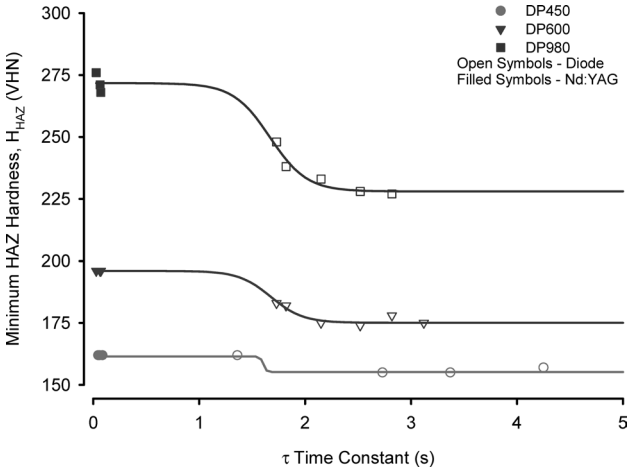

Fig. 4. Minimum HAZ hardness of DP welds made with different heat inputs resulting in different time constants at the Ac_1.

4.2. Effects of Weld Time Constant on HAZ Hardness

Using Eq. (4), all of the welding parameters were converted to time constants so that the softened HAZ hardness generated from Nd:YAG and diode laser welded material could be compared. It was found that the decrease in hardness of the DP steels studied here forms an "S" pattern where a minimum time is necessary to initiate tempering, then the HAZ softens to a minimum hardness. At this minimum hardness value the HAZ does not further decrease in hardness as the time constant increases (see **Fig. 4**). This softening pattern matches the results of previous work[6] reported a similar softening pattern in two DP600 alloys.

HAZ hardness was also rearranged to show HAZ softening by subtracting the minimum HAZ hardness from the base material hardness (see **Fig. 5**). When softening is graphed the relation between softening and time constant is

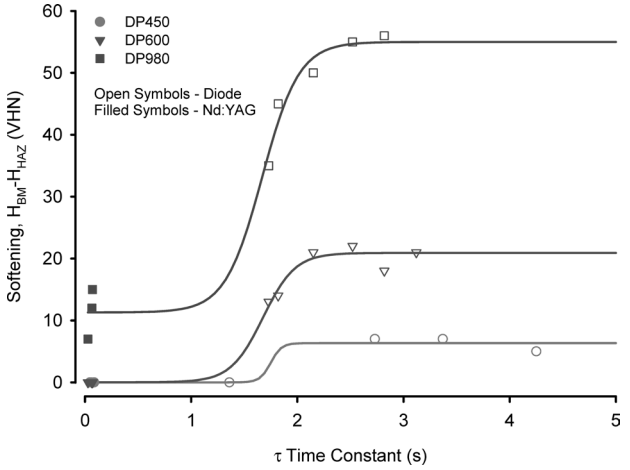

Fig. 5. HAZ softening of DP welds made with different heat inputs resulting in different time constants at the Ac_1.

inverted when compared to change of HAZ hardness with time constant. In the following discussion only HAZ softening will be referred to, which is of more interest for design of weldments than is the absolute hardness after welding.

4.3. Effects of Martensite Content on Maximum HAZ Softening

Because the ferrite phase within DP steels is not significantly altered at temperatures up to the Ac_1, it is thought that only the martensite contributes to the softening phenomenon observed in this alloy family. To confirm this assumption, limited welds were made in several additional DP steels with various martensite contents (steel details may be found in **Table 3**). To consistently compare the HAZ hardnesses all of the welds, welding parameters were chosen to ensure producing weldments with time constants ranging between 2.3–3.2 s. This ensured that the HAZ in all of the extra welds had fully softened. When the hardness profiles of these steels were measured, it was observed that the amount of HAZ softening was directly proportional to martensite content (see **Fig. 6**). This confirms that martensite content plays a dominant role in determining the maximum amount of HAZ softening when laser welding DP steels. This seems consistent with the design basis for these steels, since the volume fraction of martensite mainly determines the strength and hardness of DP steels.[2,23] As well, this result agrees with previous findings showing that the volume fraction of martensite in the DP steels determined the reduction of ultimate tensile strength when the HAZ was simulated in DP steels using a Gleeble thermal simulator.[15]

4.4. Prediction of Maximum HAZ Softening

As Fig. 6 showed that maximum softening in DP alloys is linearly related to martensite content, the softening process could be normalized for all grades by dividing the measured softening by the materials' martensite content. This parameter, as calculated below, was found to represent the softening of the martensite alone within the DP steel:

$$\Delta H_{Mart}=(H_{BM}-H_{min})/f_{Mart} \quad \text{.....(5)}$$

When martensite softening during welding is then graphed

Table 3. Diode Laser Welds with Similar Heat Inputs.

Laser	f_{mart}%	T_m (K)	T_{Ac1} (K)	Welding Speed (m/min)	$2r_{AC1}$	Minimum Hardness (VHN)	$Q_{net}/(vd)$ (J/mm^2)	τ (s)
DP450*	7.0	1804	1005	1.0	7.73	155	86.2	2.73
DP600a*	18.6	1803	993	1.4	8.55	178	86.1	2.82
DP600b	20.0	1802	992	1.0	8.27	171	85.3	2.98
DP600c	16.0	1801	1012	1.2	7.83	183	86.8	2.72
DP750	28.0	1797	997	1.4	7.49	221	79.1	2.35
DP780	28.0	1800	990	1.4	7.61	189	84.4	2.73
DP800	54.0	1797	1009	0.8	9.36	204	93.7	3.19
DP980*	49.4	1798	991	1.2	7.96	233	86.2	2.85

* Materials used previously in this study

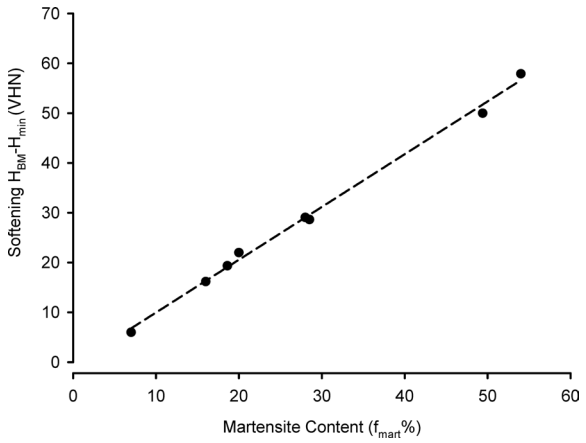

Fig. 6. Maximum amount of HAZ softening at Ac_1 ($H_{BM}-H_{min}$) *versus* martensite volume fraction.

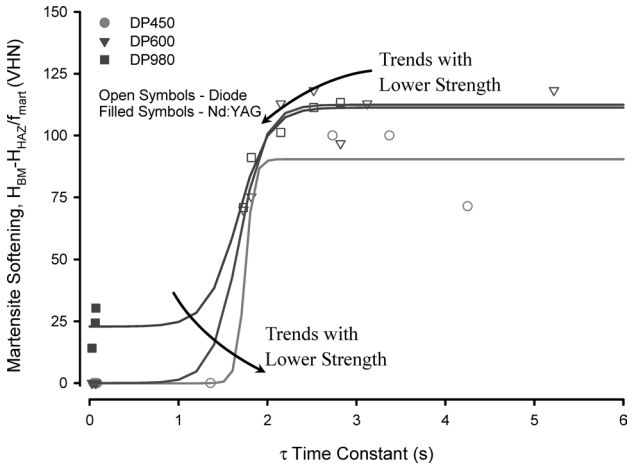

Fig. 7. Martensite softening of studied DP alloys with respect to heat input as represented by the time constant.

against the time constant, it may be seen that, as would be expected, the maximum change in martensite hardness for all three DP steels are the same. But when the "S" curves are further examined in **Fig. 7**, it may be seen that the softening kinetics for the three grades are different. In the three cases examined, the time required to initiate softening decreased with increasing strength, but lower strength DP steels fully softened before higher strength DP steels did. However it is suspected that observed changes in softening kinetics are actually controlled by material chemistry. Tempering resistance of alloy steels is well-known to be influenced by additions of different carbide-forming elements.[24] To fully understand softening kinetics a more extensive softening study should be done on a variety of DP steels with various microstructures and chemistries.

5. Conclusions

Several Nd:YAG and diode laser welds were made on DP450, DP600 and DP980 steels over a wide range of heat inputs. The HAZ softening occurring in all of these welds could be compared by evaluating the welds on a basis of time constants representing the time to heat the HAZ softened area from ambient to its Ac_1 temperature, as calculated by use of a transient thermal conduction (Rosenthal) analysis. Normalization of the tempering behaviour of all of the welds allowed several conclusions to be made about the HAZ softening phenomenon:

(1) HAZ softening occurs in an "S" pattern, needing a minimum time to initiate softening and then softening to a minimum hardness value.

(2) The total extent of HAZ softening in a DP weld at large heat input is proportional to the martensite content of the steel.

(3) The softening kinetics of the martensite may be isolated by dividing the total measured softening by the martensite content of the base material.

(4) When softening of the martensite phase is isolated from overall HAZ softening, the maximum softening for all materials were the same, but the softening kinetics differed. Higher strength materials initiated softening earlier and reached maximum softening later than lower strength DP steels.

Acknowledgement

This work was supported by Auto21 (www.auto21.ca), Dofasco, Huys Industries Ltd., Centerline Ltd., all in Canada, and International Lead Zinc Research Organization, based in USA.

REFERENCES

1) W. Bleck: *J. Met.*, **48** (1996), 26.
2) H. C. Chen and G. H. Cheng: *J. Mater. Sci.*, **24** (1989), 1991.
3) G. H. Thomas and M. X. Chen: *Iron Steelmaker* (*USA*), **29** (2002), 27.
4) T. Taka, K. Kunishige, N. Yamauchi and N. Nagao: *ISIJ Int.*, **29** (1989), 503.
5) P. K. Ghosh, P. C. Gupta, R. A. M. Avtar and B. K. Jha: *ISIJ Int.*, **30** (1990), 233.
6) E. Biro and A. Lee: Sheet Welding Conf. XI, AWS, Miami, FL, (2004), 5-2.
7) B. Hartley and M. Ono: SAE 2002 World Cong. & Exhibition, SAE, Warrendale, PA, (2002), 2002-01-0150.
8) M. Xia, N. Sreenivasan, S. Lawson, Y. Zhou and Z. Tian: *J. Eng. Mater. Technol.*, **129** (2007), 446.
9) T. Waterschoot, K. Verbeken and B. C. D. Cooman: *ISIJ Int.*, **46** (2006), 138.
10) A. Joarder, J. N. Jha, S. N. Ojha, and D. S. Sarma: *Mater. Charact.*, **25** (1990), 199.
11) B. K. Jha, R. Avtar, V. S. Dwivedi and N. S. Mishra: *Steel Res.*, **64** (1993), 171.
12) M. S. Rashid and B. V. N. Rao: *Metall. Trans. A*, **13A** (1982), 1679.
13) G. R. Speich, A. J. Schwoeble and G. P. Huffman: *Metall. Trans. A*, **14A** (1983), 1079.
14) R. G. Davies: Proc. of Symp. 110th AIME Annu. Meet., AIME, Warrendale, PA, (1981), 265.
15) E. Biro and A. Lee: Sheet Welding Conf. XII, AWS, Miami, FL, (2006), 7-1.
16) G. F. Vander Voort: Metallography Principles and Practice, McGraw-Hill, Inc., New York, (1984), 637.
17) N. Yurioka, H. Suzuki and S. Ohshita: *Weld. J.*, **62** (1983), 147s.
18) C. M. Smithells: Metal Reference Book, 5th ed., Butterworths, London, (1976), 510.
19) N. Yurioka: Weldability Calculation, http://homepage3.nifty.com/yurioka/. (accessed September, 2007)
20) J. C. Ion, K. E. Easterling and M. F. Ashiby: *Acta Metall.*, **32** (1984), 1949.
21) M. F. Ashby and K. E. Easterling: *Acta Metall.*, **30** (1982), 1969.
22) Ø. Grong: Metallurgical Modelling of Welding, Institute of Materials, London, (1994), 1.
23) A. B. Cota, F. L. G. Oliveira and A. L. R. Barbosa: *Mater. Res.*, **6** (2003), 171.
24) E. C. Bain and H. W. Paxton: Alloying Elements in Steel, 2nd ed., Third Revised Printing, ASM, Materials Park, OH, (1966), 37.